Neutron Properties in the Nuclear Medium Studied by Polarization Measurements

Letter of Intent to JLab PAC 35

G. Ron (spokeperson) [1]

Lawrence Berkeley National Lab, Berkeley 94720, USA

R. Gilman (spokesperson)

Rutgers, The State University of New Jersey, Piscataway, New Jersey 08854, USA

S. Strauch (spokesperson)

University of South Carolina, Columbia, SC, USA

O. Chen, I. Kolover, J. Lichtenstadt (spokesperson), E. Piasetzky, I. Pomerantz, and R. Shneor

Tel Aviv University, Tel Aviv, 69978 Israel

H. Areti, D.W. Higinbotham (spokesperson), and B. Sawatzky

Thomas Jefferson National Accelerator Facility, Newport News, VA 23606, USA

I. Cloet and G. A. Miller

University of Washington, Seattle, WA, USA

J. Watson

Kent State University, Kent, Ohio 44242, USA

S. Gilad, V. Sulkosky, and X. Zhan

Massachusetts Institute of Technology, Cambridge, MA 02139, USA

A. Beck and S. Maytal-Beck

Nuclear Research Center Negev, P.O.Box 9001, Beer-Sheva, Israel

K. Allada

University of Kentucky, KY, USA

K. Slifer

University of New Hampshire, Durham, NH, USA

Abstract

Objective: In the quark-model picture of the nucleon, a free nucleon placed in the strong field of the nucleus has its structure modified. The nuclear-medium modifications of the nucleon are expected to affect the ratio of the bound neutron electric to magnetic form-factor ratio G_E^*/G_M^* in comparison to that of the free neutron G_E/G_M . The ratio of these quantities at low momentum transfer depends on the neutron magnetic moment and its charge distribution effective radius. This ratio is expected to be very different in the case of the proton, thus comparison of the behavior of the double ratio $\frac{G_E^*/G_M^*}{G_E/G_M}$ of both the proton and the neutron sheds light on the nuclear-modification mechanisms at work.

Methodology: The double ratio of neutron-recoil polarization-transfer coefficients $P_x'^*$ and $P_z'^*$ of the quasi-elastic reaction $^4\mathrm{He}(\vec{e}, e'\vec{n})^3\mathrm{He}$ with respect to the $d(\vec{e}, e'\vec{n})p$ reaction (where the knock-out neutron was only loosely bound in the target) is sensitive to possible medium modifications of the electric and magnetic form factors. The double ratio $\frac{P_x'^*/P_z'^*}{P_x'/P_z'}$ be determined by measuring the polarization transfer components of the knock-out neutron in polarized electron quasielastic scattering in the $^4\mathrm{He}(\vec{e}, e'\vec{n})^3\mathrm{He}$ and $d(\vec{e}, e'\vec{n})p$ reactions. In addition, the normal component of the induced polarization P_y imposes additional constraints on the proposed mechanisms, and will be measured as well. We propose to perform the measurement at Hall C at beam energies of 2.2 and 6.6 GeV, at 2 Q^2 values, 0.1 and 0.4 GeV^2, the experiment will use a neutron polarimeter to be designed and built and the SHMS spectrometer.

Significance: Various mechanisms have been proposed to explain nuclear medium modifications of the nucleon. Some are attributed to nuclear modification of the scattering

[1] contact person: Guy Ron, gron@jlab.org

process while others suggest modifications in the nucleon structure like its radius, the quark momentum distribution etc. The data on the neutron along with existing data on the proton will provide important information to distinguish between the two classes of modification mechanisms.

1 Scientific background

It is well known that, to a very good approximation, nuclei can be described as systems of nucleons in a mean field. However, nuclear properties are modified in the nuclear medium. A trivial example is the change in the lifetime of the neutron, from approximately 15 min to infinity, when bound in stable nuclei. It is a major challenge of modern nuclear physics to identify and study these non trivial, small, but important, modifications of a single nucleon due to its presence in the nuclear medium. A well known example of such a change between a bound and free nucleon is the well established *EMC effect* [1–7], where the cross section for deep inelastic scattering off a nucleon bound in a nucleus is reduced relative to that of a free nucleon [8,9] (and references therein).

The interpretation of the EMC effect within the parton model, is that the valence quarks in a nucleon bound in a nucleus carry less momentum than in the free nucleon. The uncertainty principle then implies that the nucleon's size may also increase [8,10,11].This medium modification of nucleon structure should have consequences for nuclear reactions that are sensitive to the properties of a single nucleon. However, unambiguous evidence for such modifications has not yet been observed.

Modifications of bound nucleons relative to free nucleons have been suggested as explanations for other observed phenomena, such as, the quenching of the axial form factor [12], quenching of the Coulomb Sum Rule (CSR) [13], and deviation of low momentum K^+ total cross section ratios from calculations [14,15]. Recently the in-medium modification of nucleons was also proposed [16] as a possible explanation to the NuTeV anomaly [17].

Theory has not come up yet with unequivocal explanation of these phenomena. In general, two classes of explanations have been proposed. The first is effects stemming from the nuclear structure, for example, non-nucleonic degrees of freedom in the nucleus causing enhancement of quark-antiquark pair populations [18–21]. A second class of explanations considers modifications in the fundamental structure of the nucleon by the influence of the external nuclear medium on the nucleon wavefunction. Among these are *Dynamical Rescaling Models* [22–24] which suggest a change in the quark confinement scale due to the effects of the nuclear color charge, leading to what is sometimes referred to as a *"nucleon swelling"*.

The elastic scattering of an electron off a finite size nucleon can be expressed using elastic form factors by the Rosenbluth formula:

$$\frac{d\sigma}{d\Omega} = \frac{\alpha^2}{Q^2}\left(\frac{E}{E'}\right)^2\left(\frac{\cot^2\frac{\theta_e}{2}}{1+\tau}\left[G_E^2+\tau G_M^2\right]+2\tau G_M^2\right) \tag{1}$$

Where α is the fine structure constant, Q^2 is the negative of the square of the four momentum transfer, E and E' are incident and scattered electron energies respectively, $\tau = Q^2/4M^2$, M is the nucleon mass, and G_E and G_M are the nucleon elastic form factors, normalized according to:

$$G_E^p(0) = 1,\ G_M^p(0) = \mu_p, \tag{2}$$
$$G_E^n(0) = 0,\ G_M^n(0) = \mu_n, \tag{3}$$

where $\mu_p \sim 2.793$ ($\mu_n \sim -1.91$) is the proton (neutron) anomalous magnetic moment.

The polarization transfer reaction $(\vec{e}, e'\vec{p})$ on a proton target measures quantities proportional to the ratio of the proton's electric and magnetic form factors [25]. When performed on a nuclear target, (*e.g.* $^4\mathrm{He}\,(\vec{e}, e'\vec{p})\,^3\mathrm{H}$), the measured polarization-transfer observables are sensitive to the G_E/G_M form factor ratio of a proton embedded in the nuclear medium.

Several authors have suggested [26–28] that polarization measurements of knockout nucleons may present a method of discriminating between the two classes of models for medium modification. In general, polarization components of the recoil (free) nucleon are related to the charge and magnetization densities of the nucleon and should be little affected by non-nucleonic degrees of freedom such as meson exchange currents. Thus, their modification in nuclei may suggest a change in the nucleonic structure.

Several polarization-transfer proton-knockout experiments have been performed on ^{4}He, both at the MAMI facility [29] and at JLab [25,29]. Fig 1 shows preliminary results of the double-ratio of the in-plane polarization components in ^{4}He and a free proton $(P'_x/P'_z)_{^4\mathrm{He}}/(P'_x/P'_z)_{\mathrm{H}}$, which reflects the changes in the double ratio of the corresponding double ratio of the electric and magnetic form factors, obtained from polarization transfer measurements, compared to a calculation in PWIA.

The figure shows a reduction of the double-ratio between experimental ratio and the calculation which is consistent with models which consider modifications of the nucleon structure [30,31]. As shown, the data can be described well by including the effects of

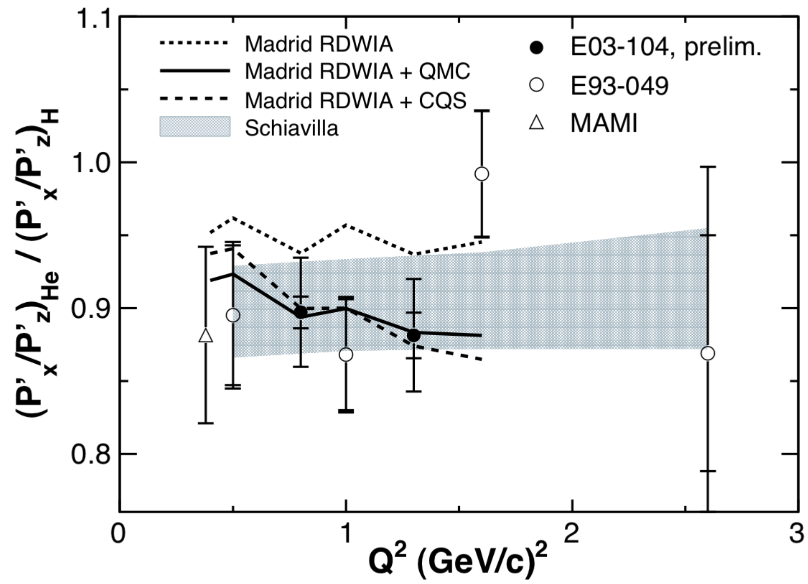

Fig. 1. Preliminary results for the double-ratio of polarization components of a bound proton (in ^{4}He) to a free one for experiments E03-104 (full circles), E93-049 (empty circles), and the MAINZ experiment (triangles). The curves represent a Udias RDWIA calculation with QMC (solid), CQS (dashed), and no (dotted) contributions, and a full relativistic model from Schaivilla *et al.* (grey band) which takes into account a spin-dependent charge exchange final state interaction.

medium-modified form factors [30,32–36] but also by including effects from strong charge-exchange final state interactions (FSI) [37]. However, the effects of the strong FSI may not be consistent with measurements of polarization transfer to the knockout nucleon [25]. As seen in Fig. 2, calculations which produced well the form factor ratio by including medium effects on the scattering process seem to over-estimate the 'normal' component of the polarization transfer to the knockout nucleon P_y measured at JLab, indicating that corrections of the nucleon properties should be considered as well.

An indication of the existence of FSI effects may be seen in the induced polarization component of the recoil nucleon (see 3.1), a Q^2 dependence of the induced polarization is a strong indication of such effects, as well as any strong deviation from zero. Figure 2 shows the induced polarization component of the recoil proton, as measured at JLab, evidently, the figure shows disagreement between the measured polarization and the calculated value in a theoretical model which includes charge exchange FSI [37] (magenta dotted).

Measurements of polarization transfer in *neutron* knockout reactions like $^4\mathrm{He}\,(\vec{e}, e'\vec{n})\,^3\mathrm{He}$ will add important information on the nuclear medium mechanisms at work, and identify modifications of the nucleon structure.

To demonstrate the difference between proton and neutron modifications in the nucleus

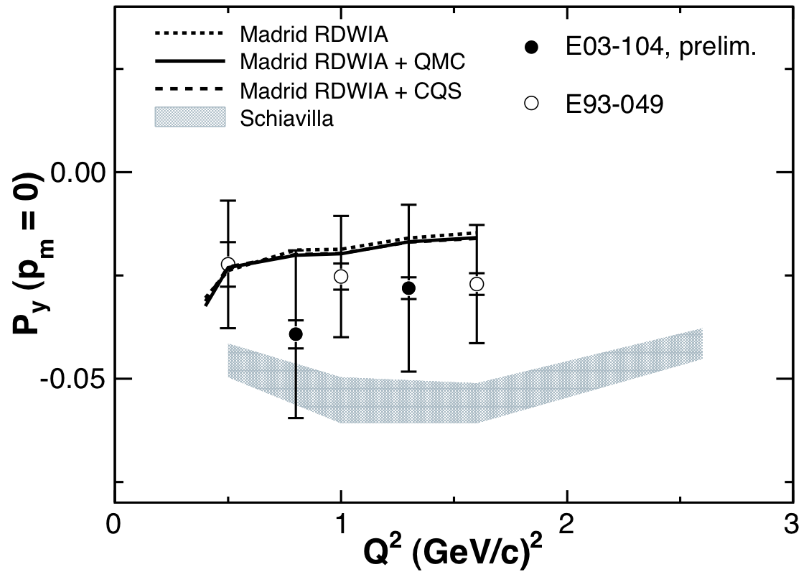

Fig. 2. Preliminary results for the induced polarization P_y versus Q^2. Curves and data points are the same as for Fig. 1.

we consider the situation at small values of Q^2. In this region the Sachs form factors for the free proton can be expressed in the form

$$G_{Ep}(Q^2) \simeq 1 - \tfrac{1}{6}\, Q^2\, \hat{R}^2_{Ep}, \tag{4}$$

$$\frac{1}{\mu_p} G_{Mp}(Q^2) \simeq 1 - \tfrac{1}{6}\, Q^2\, \hat{R}^2_{Mp}, \tag{5}$$

where $\hat{R}_{Ep}$ and $\hat{R}_{Mp}$, are the effective electric and magnetic radii respectively [38]. Keeping only the leading Q^2 dependence, the proton electric to magnetic form factor ratio can be expressed as

$$\mathcal{R}_p \equiv \frac{G_{Ep}(Q^2)}{G_{Mp}(Q^2)} \simeq \frac{1}{\mu_p} \left[1 - \tfrac{1}{6}\, Q^2 (\hat{R}^2_{Ep} - \hat{R}^2_{Mp})\right]. \tag{6}$$

For a bound proton we may define an analogous ratio which we label $\mathcal{R}^*_p$. The influence of the medium may change any of the three quantities μ_p, $\hat{R}_{Ep}$ and $\hat{R}_{Mp}$. Extensive studies of the EMC effect suggest that the nucleon expands in the nuclear medium. Since $\hat{R}^2_{Ep} \simeq \hat{R}^2_{Mp}$ in a free proton, and in-medium effects should be similar for the electric and magnetic radii, one expects a negligible Q^2 term in Eq. (6). On the other hand, one may expect that the value of μ_p in the medium will increase, along with the increasing magnetic radius. In this scenario the double-ratio $\mathcal{R}^*_p/\mathcal{R}_p$ would be less than one and largely independent of

Q^2. This is consistent with the measurements as can be seen in Fig 1 and in Refs [25,27].

To help resolve the different mechanisms responsible of the medium modification and determine the influence of FSI we consider the neutron in the nuclear medium. The analogous expression to Eq. (6) for the neutron, valid at small Q^2, is

$$\mathcal{R}_n \equiv \frac{G_{En}(Q^2)}{G_{Mn}(Q^2)} \simeq -\frac{1}{\mu_n}\,\frac{1}{6}\,Q^2\,\hat{R}_{En}^2, \tag{7}$$

where the effective magnetic radius does not appear, since it is the coefficient of a Q^4 term. In contrast to the proton, the medium modifications are expected to depend generally on possible changes in both the electric radius and magnetic moment. This implies that the the double-ratio $\mathcal{R}_n^*/\mathcal{R}_n$ should increase at small Q^2 due to the expected increases of both these quantities. Since the electric radius contribution (Eq. (7)) enters quadratically one may expect, in contrast with the proton, that the neutron double-ratio will be larger than one and show a Q^2 dependence.

These expectations are borne out by specific model calculations [39]. In the quark-diquark model, Nambu–Jona-Lasinio (NJL) [34,36], predict that both $\hat{R}_{En}$ and $\hat{R}_{Mn}$ increase in the nuclear medium. However, there is only a small change in the neutron magnetic moment. Therefore at low Q^2 the double-ratio $\mathcal{R}_n^*/\mathcal{R}_n$ is dominated by the change in $\hat{R}_{En}$ and is expected to increase. This is shown in Fig. 3 where the results of Ref. [36] are illustrated. In the model of Smith & Miller [32] the value of μ_n and $\hat{R}_{Mn}$ are essentially unchanged in the medium, but $\hat{R}_{En}$ is predicted to increase. Therefore both models predict that the double-ratio increases for the neutron and decreases for the proton.

2 Research objective and expected significance

An intriguing question in nuclear physics is understanding where the quark and gluon degrees of freedom become important to understanding the structure and properties of nuclei, which to a good approximation are described as a system of nucleons in a mean field. Explanations of the EMC effect in nuclei suggest that the momentum distribution of quarks in the valence region of bound nucleons, differs from that of quarks in a free nucleon. In spite of the major advances in both the experimental and theoretical arenas, there is as yet no consensus concerning the origin of the effect and attributing it to specific structure modifications of bound nucleons. The objective of this proposal is to experimentally test theoretical predictions of modifications of the nucleon structure in the nuclear medium in comparison to that of a free nucleon by measurements on the neutron.

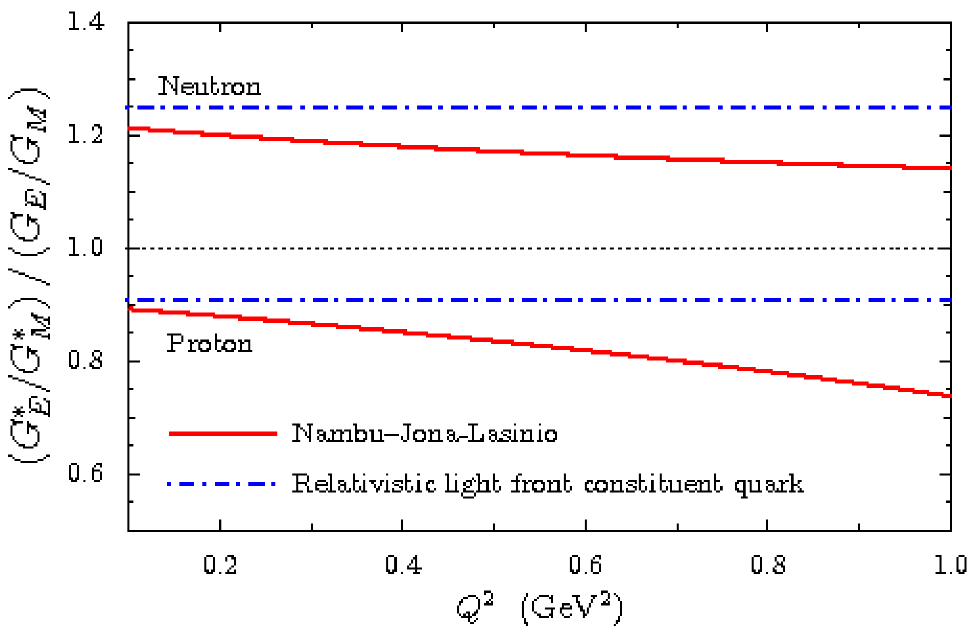

Fig. 3. Double-ratios for the neutron and proton form factors obtained from the Nambu–Jona-Lasinio model of Ref. [36] and the relativistic light front constituent quark model of Ref. [40].

3 Detailed description of the proposed research

3.1 The proposed measurement

The ratio of the neutron electric and magnetic form factors will be determined from measurement of the polarization of knocked-out neutrons by polarized electrons.

The coordinate system of the knockout reaction is illustrated in Fig. 4. where $\vec{k}$ ($\vec{k'}$) is the incident (scattered) electron momentum, $\vec{q} = \vec{k} - \vec{k'}$ is the momentum transfer vector, and p_A, p' and p_{A-1} are the momenta of the target nucleus, the knocked-out nucleon and the residual nucleus respectively. The components of the polarization vector (due to polarization transfer from the longitudinaly polarized electron) are defined as: P'_z the component parallel to the nucleon momentum, P'_x the transverse polarization component in the scattering plane, and P_y, the polarization component normal to the scattering plane.

The relation between the polarization components of a *free nucleon* and the form factors can be written as [41–43]:

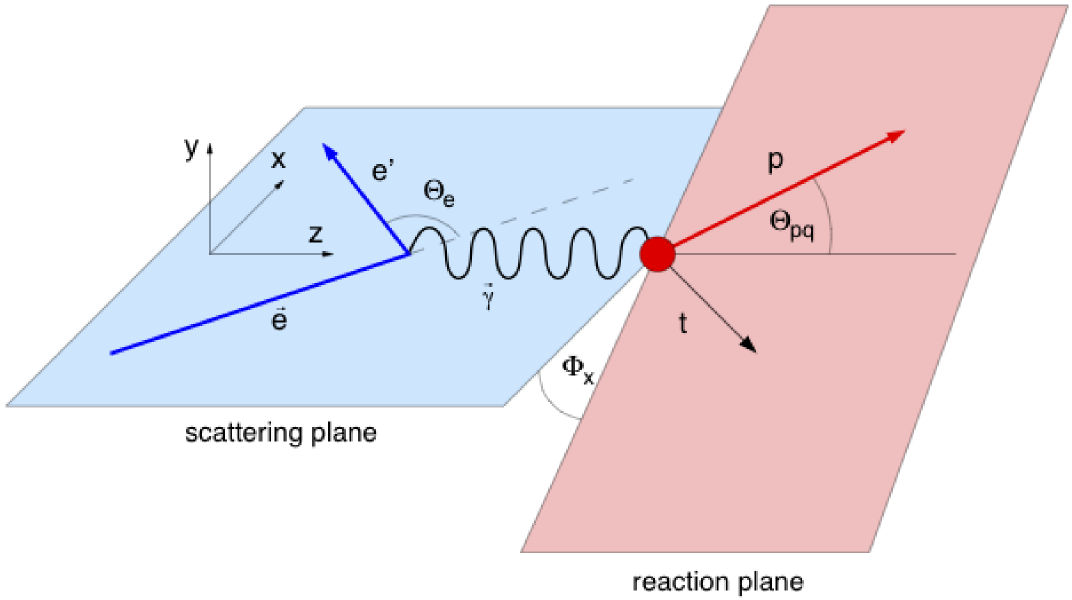

Fig. 4. Coordinate system and polarization components for the recoil polarization measurement in quasi-free scattering.

$$\sigma_{red} P'_x = -2\sqrt{\tau(1+\tau)} \tan\frac{\theta_e}{2} G_E G_M, \tag{8}$$

$$\sigma_{red} P'_z = \frac{E+E'}{M_p}\sqrt{\tau(1+\tau)} \tan^2\frac{\theta_e}{2} G_M^2, \text{ and} \tag{9}$$

$$P_y = 0, \tag{10}$$

where σ_{red} is the reduced cross section, and P'_x (P'_z) is the transverse (longitudinal) in-plane polarization component in the scattering frame. For a single (virtual) photon exchange (the *Born approximation*) the normal component of the polarization, P_y, is identically zero.

In order to determine the effects of medium modifications on the polarization components of the recoil neutron the reaction ^{4}He$(\vec{e}, e'\vec{n})^3$He will be utilized. The density of the ^{4}He nucleus is high, and its structure is simple and described well by the shell model (one should note however, the effects of integration over the non-constant nuclear density when calculating the modified form factors). It is worth noting that a recent measurement from Hall C of the EMC effect in light nuclei [7] found the effect in ^{4}He to be almost as large as that in ^{12}C. In order to compare the results to those of a free neutron we plan to use the reaction ^{2}H$(\vec{e}, e'\vec{n})$p. Due to the low density and small binding energy of the deuteron it can be used as a simulacrum of a free neutron.

The polarization components of the recoil neutron will be measured from the asymmetry (analyzing power) in the $p(\vec{n}, X)$ polarized neutron scattering reaction off the hydrogen nuclei in scintillating bars which will comprise the neutron polarimeter, and will serve also as the neutron detector. The spin orbit interaction between the neutron and the hydrogen nucleus and the spin dependent asymmetry in the scattering cross section result in an angular distribution of the scattering cross section. The measured angular distribution of the secondary scattering reaction (for both elastic and charge-exchange processes, normalized to the total number of counts N_0) can be written as:

$$f(\theta,\phi)=\frac{1}{2\pi}\left[1-A_y(\theta,T_n)P_x\sin\phi+A_y(\theta,T_n)P_y\cos\phi\right], \tag{11}$$

where the analyzing power, A_y, depends on the polar angle θ_n and the neutron kinetic energy. Note that the polarization components measured are in the secondary scattering reaction frame and must be rotated accordingly to determine P_y, P'_x and P'_z which are, as noted, in the initial scattering frame.

In reality, both neutron polarization components are multiplied by the beam helicity and polarization h. Thus, one may define two sets of distributions f^+ and f^- for the two beam helicity states. By measuring the two helicity distributions it is then possible to subtract the two distributions,

$$f^{\text{diff}}(\theta,\phi) = f^+ - f^- = \frac{1}{\pi}A_y(\theta,T_n)\left(P_y\cos\phi - P_x\sin\phi\right). \tag{12}$$

From Eq. (11) it is can be seen that the np reaction is not sensitive to the longitudinal component of the neutron spin polarization. This is due to the orthogonality of the angular momentum and the longitudinal spin component of the neutron. In order to measure the longitudinal spin component the spin vector must be rotated by making use of an analyzing magnet which rotates the neutron spin vector according to:

$$\chi = \frac{\mu_n}{\beta_n}\int |\mathbf{B}|dl, \tag{13}$$

where β_n denotes the neutron velocity, and B the magnetic field. Since, in general, FSI effects may induce a normal polarization component, this experiment (unlike experiments on free protons) requires a measurement of all three polarization components (in order to compare with FSI calculation) and hence must use at least two magnet settings for each measurement.

The strength of the recoil polarization technique is further evident when considering that the measurement performed is for the ratio of polarization components. Using Eq. (12) it is possible to extract the products $A_y P_x$ and $A_y P_y$. However, when taking the ratio of these quantities the analyzing power, A_y, cancels out and the calculated value is simply P_x/P_y. In general, when using a vertical field dipole magnet to precess the neutron spin vector by some angle χ, the polarization components in the polarimeter frame are given by:

$$\begin{pmatrix} P_x \\ P_y \\ P_z \end{pmatrix} = \begin{pmatrix} \cos\chi & 0 & \sin\chi \\ 0 & 1 & 0 \\ -\sin\chi & 0 & \cos\chi \end{pmatrix} \begin{pmatrix} P'_x \\ P_n \\ P'_z \end{pmatrix} . \tag{14}$$

Giving for f^{diff}:

$$f^{diff} = \frac{1}{\pi} A_y \left[- \left(P'_x \cos\chi + P'_z \sin\chi \right) \sin\phi \right] . \tag{15}$$

By setting $\chi = \pm 45°$ it is possible to extract all three polarization components using two field settings. In each of the different field settings one extracts the induced polarization, P_y, as well as a linear combination of P'_z and P'_x. The two different extractions of P_y then serve as a consistency check, and the two linear combination measurements are used to obtain $A_y P'_x$ and $A_y P'_z$ and the ratio P'_x/P'_z.

It should be noted that misalignments and non-uniform efficiencies in the detector may introduce false asymmetries. To approximately account for such contributions, Eq. (11) should be modified to read:

$$\begin{aligned} f(\theta,\phi) = \frac{1}{2\pi} & \left[1 + (a_0 - A_y(\theta, T_n) P_x) \sin\phi + (b_0 + A_y(\theta, T_n) P_y) \cos\phi \right. \\ & \left. + c_0 \cos(2\phi) + d_0 \sin(2\phi) \right] , \end{aligned} \tag{16}$$

where a_0, b_0, c_0, d_0 account for possible false asymmetries. However, since the false asymmetries are independent of the beam helicity leaving the angular distribution of the difference (12) unchanged. It is also possible to determine the false asymmetries by summing the helicity distributions,

$$f^{sum} = f^+ + f^- = \frac{1}{\pi} \left[a_0 \sin\phi + b_0 \cos\phi + c_0 \cos(2\phi) + d_0 \sin(2\phi) + A_y P_y \cos\phi \right] , \tag{17}$$

and fit for the false-asymmetry terms. In addition, using a deuteron target, to measure these asymmetries for a 'free' neutron we get additional information on possible false asymmetries. It is possible then to extract the false-asymmetry terms for the ^{2}H($\vec{e},\vec{n}$)p reaction and use them to test for final state interactions in the ^{4}He reaction (since for a free nucleon $P_y = 0$ (Eq. (10)).

Several problems must be addressed when performing the measurement of the neutron medium modified form factors and the comparison to theoretical calculations.

Final State Interactions

A main concern in the measurement is the charge exchange final state interaction reaction. Fig. 7 shows the cross section ratio (using the parametrization from [44]) for elastic electron scattering off a free proton to a free neutron. Since for low Q^2 the cross section is dominated by the electric form factor (see Eq. (1)) and the neutron electric form factor is much smaller than the proton electric FF we expect a certain fraction of detected recoil neutrons to be generated via the charge exchange reaction $\vec{p}(n,\vec{n})$ in the nucleus.

In principle, such effects must be understood if one is to perform an accurate comparison of the free to bound form factor ratio. However, several calculations have shown (see [45]) using different optical potentials did not change the overall effect significantly, furthermore, new state-of-the-art few body calculations allow to calculate the interaction to several percent accuracy, giving overall a manageable uncertainty budget from FSI. Note, that since the normal polarization is completely dependent on FSI effects, the measurement of that polarization component will help constrain the FSI effects in any model used.

Another noteworthy fact is that while for the case of the proton a distortion of the recoil proton wavefunction in the Coulomb field of the residual (^{3}H) nucleus must be taken into account (see for eg. [46]) for the uncharged neutron such interaction is minimal and only the (short-range) hadronic and magnetic moment interactions must be taken into account, further suppressing FSI effects.

Missing energy resolution

In order to calculate the interaction with the residual (^{3}He) the data must be selected such that the events analyzed are those in which the residual nucleus is in the ground state. Fortunately, the ^{3}He nucleus has no excited bound states, transitioning to the $d+p$ and the continuum states with a binding energy of $\sim$ 7.7 MeV. Thus, selection of events with missing energy less than 7.7 MeV will guarantee a definite final state for the residual nucleus. Assuming a neutron detector placed 7 m from the target and a time resolution of 300 ps it is possible to estimate the missing energy resolution as a function of Q^2 using a MC simulation which takes into account finite detector acceptances and resolution (assuming 10 cm $\times$ 10 cm detectors at 7 m). Table 1 shows the simulated missing mass resolution for several Q^2 values.

Beam polarization drift

Since for each kinematic settings 4 measurements of the neutron polarization components must be performed, 2 magnet settings each for scattering off a ^{2}H and a ^{4}He, the extraction of the double-ratio must take into account the possible different beam polarization at each of the different measurements (this is not the case for proton polarization measurements in which only one magnet setting is used). Note, however, that only the *relative* polarization change between different measurements must be known, since the absolute polarization scale is cancelled in the ratio.

Beam polarization measurements are typically performed on-line using a Compton or Moller polarimeter installed upstream of the target. Typical relative uncertainties in the bean polarization measurement are $\sim$1%, having a negligible effect on the extraction of the medium modified double-ratio.

3.2 Polarimeter design and construction

Fig 5. shows the polarimeter design as proposed for a measurement of the neutron electric form factor up to Q^2 of 7 GeV^2 using recoil polarimetry [47]. This design is an improvement on a polarimeter used to measure G_E^n at JLab [48] using the same (Charybdis) analyzing magnet. Neutrons are scattered in the front scintillator array. The asymmetry is measured in the up/down direction only by the rear scintillator array. The dipole magnet upstream precesses the neutron polarization vector and allows measurements of both P'_x and P'_z as discussed above. This design does not allow the determination of the normal component of the induced polarization, P_y which was shown to impose an important test of the proposed nuclear-medium modification-mechanism in the case of the proton [37]. To allow for a measurement of P_y we propose to add to the design two more Left and Right rear arrays.

We also consider a more symmetric design, shown schematically in Fig. 6, following a conceptual design used with a low energy neutron beam at the Indiana accelerator [49]. The upstream dipole magnet is followed by a front detector for neutron detection and analyzing and a cylindrical detector for the asymmetry measurement. The fact that the neutrons enter along the length of the front neutron detectors allows us to set a very high detection threshold, reducing substantially the background rates.

The front and rear detectors are in a shielded bunker [48]. We propose to build a bunker large enough so that it will be possible to move the detectors situated inside by several degrees to allow the two kinematical setups described below.

The rear detector will be constructed as to be a variable distance from the front detector in order to allow optimization of the energy deposit of the secondary scattering in the front detector and optimization of the analyzing power of the secondary scattering reaction (both of which are polar angle dependent).

Studying and selecting the both designs and as well as optimization of the detector parameters require extensive study, which will be performed as part of this research.

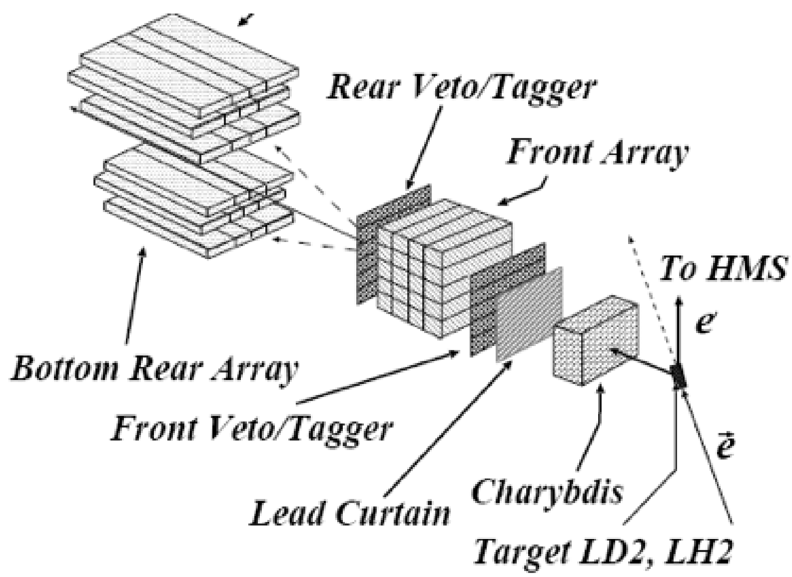

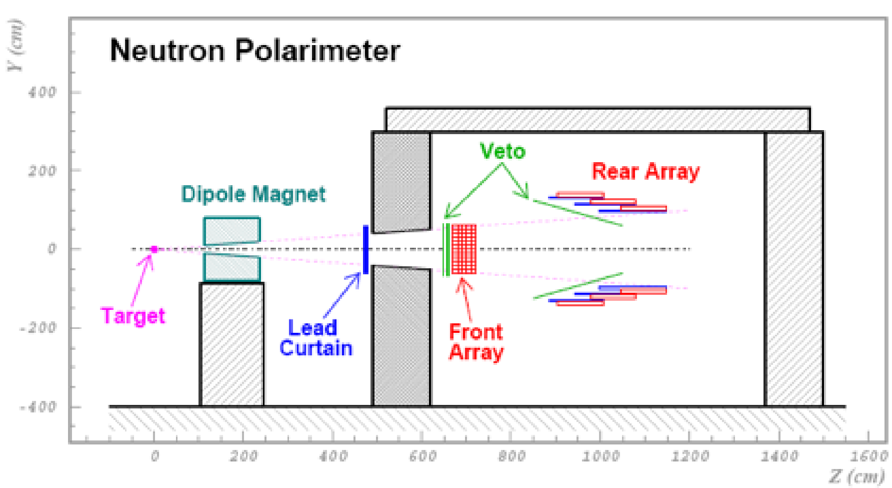

Fig. 5. The polarimeter design proposed for PR09-006. Our first prototype will be similar to this design and add two rear arrays to the left and right sides of the beam.

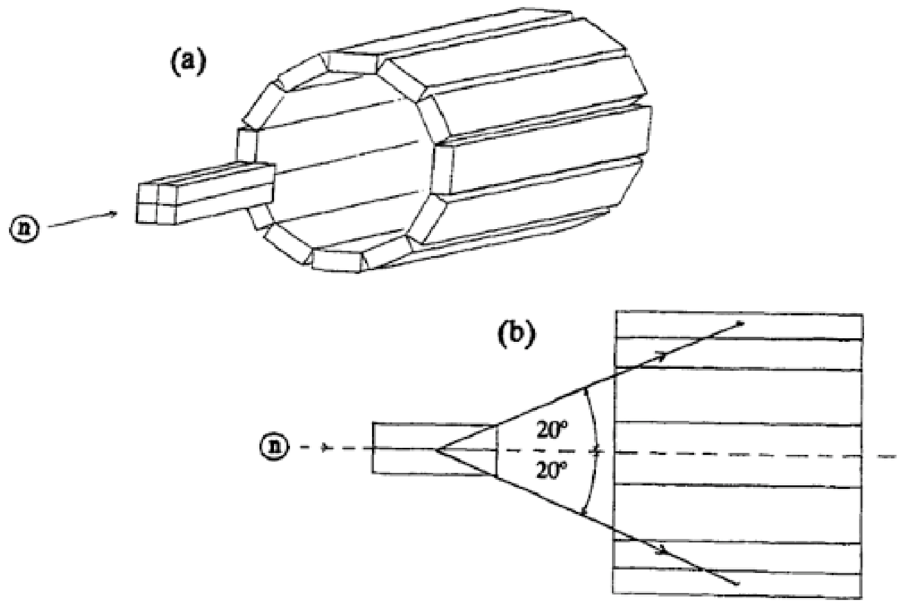

Fig. 6. The "2π neutron polarimeter. (a) Isometric view. (b) From above.

3.3 The selected kinematics for the measurement

Unfolding the nuclear dynamics in order to extract the single nucleon form factors from electron scattering experiments is a complicated task due to the following reasons:

- The inherent uncertainties in the nuclear Hamiltonian and currents,
- The need to solve the nuclear many-body problem in the continuum, and
- Relativistic corrections.

However, at relatively low momentum transfer ($q < 600$MeV/c) this task becomes somewhat simplified as the accuracy of the nuclear Hamiltonian and currents can be put under control through the effective field theory (EFT) low momentum expansion. Relativistic corrections have only minor effect, and the nuclear dynamics can be solved quite accurately. Recently it was demonstrated that through the combination of the Lorentz Integral transform approach (LIT) [50,51] and the effective interaction hyperspherical Harmonics method (EIHH) [52] the inclusive inelastic electron scattering on ^{4}He can be resolved to a percentage accuracy [53]. This result infers that a similar accuracy can be achieved for other 4–body reactions such as the neutron polarization experiment discussed above.

In short, the combination of modern nuclear forces and currents together with the LIT and EIHH resolution methods allows for a controlled estimate of the nuclear rule in the electron scattering on ^{4}He and therefore contstraining the single nucleon form factors.

We thus identify several kinematics in which we suggest to perform the measurements. Table 1 details the suggested kinematics. We now describe the reasoning behind each of the selected kinematics:

- $Q^2 = 0.1$ GeV^2 - The lowest easily accessible Q^2 point will allow the best theoretical calculation of the response function and the FSI effects. Furthermore, this measurement will also provide a constraint on the neutron form factors (from the scattering off the deuteron) in a momentum transfer regime where such measurements are scarce.
- $Q^2 = 0.4$ GeV^2 - At this Q^2 value the neutron electric form factor attains a maximum value, where it's derivative is equal to zero. Recall that the effective radius is defined [39] as the derivative of the form factor. Thus, at this momentum transfer one has maximum sensitivity to effects from the magnetic form factor (changes in the magnetic charge radius) in the nucleus. Also, a possible (even probable) consequence of the change in the charge radius in the medium will be a shift in the position of the maximum of the form factor. Such a shift will manifest in a structure in the double ratio caused by the different behavior of the free and bound form factors.

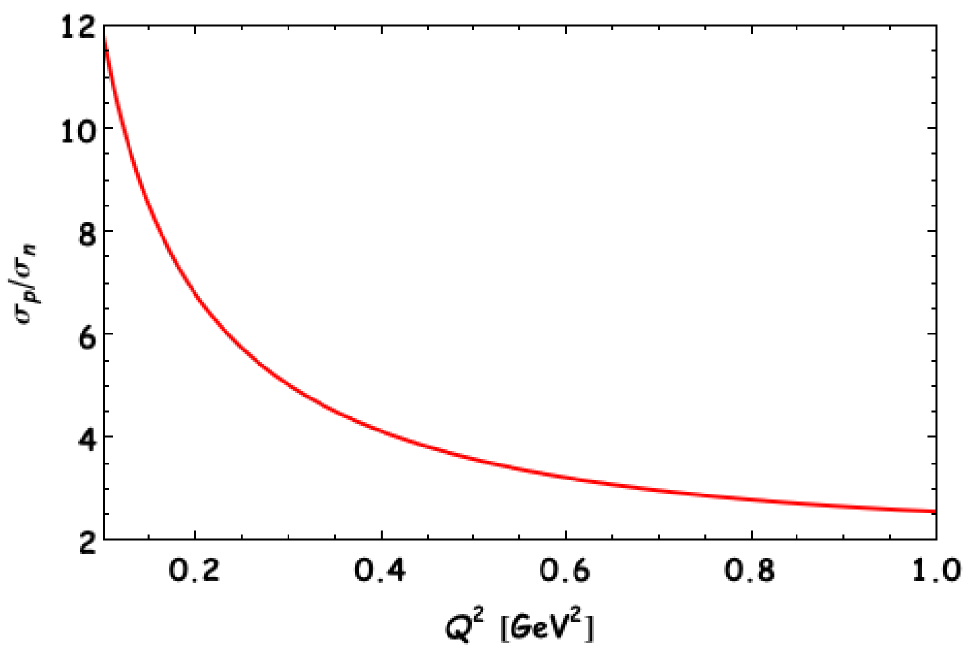

Fig. 7. Ratio of proton to neutron elastic cross sections for 2.2 GeV beam energy as a function of Q^2.

Q^2 (GeV^2)	E_{Beam} (GeV)	ΔM_{miss} (MeV)	T_n (MeV)	$\|\vec{q}\|$ (MeV)	θ_n (deg)	θ_e (deg)
0.1	2.2	1.7	53.2	320.6	76.3	8.3
0.4	6.6	3.2	212.8	667.3	68.6	5.58

Table 1

Missing mass resolution and kinematics for several selected Q^2 values.

Figure 8 shows results of the simulations for the missing mass resolution (plotted as $M_{miss} - M_{^3He}$) for $Q^2 = 0.1$ GeV^2 (top) and, 0.4 GeV^2 (bottom).

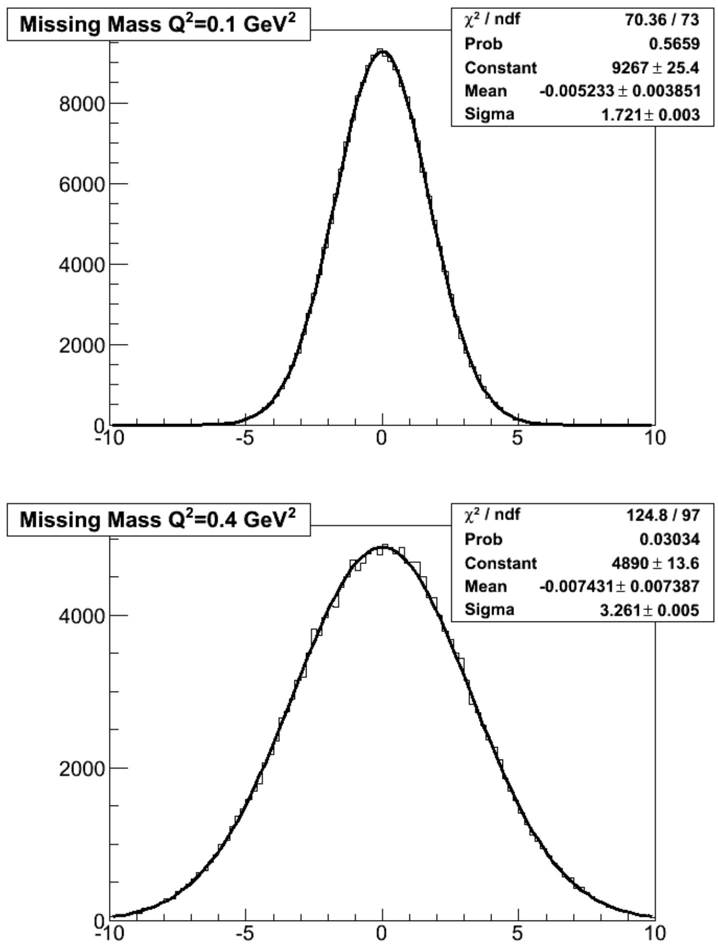

Fig. 8. Missing mass simulation for $Q^2 = 0.1$ GeV^2 (top), 0.4 GeV^2 (bottom).

3.4 Description of the experiment

The measurement is proposed for the JLab facility at the 12 GeV era using the 2.2 and 6.6 GeV (1 and 3 pass) beams. The electron will be detected with the Hall C SHMS spectrometer while the neutron will be detected in coincidence using a dedicated neutron detector/polarimeter.

4 The proposed measurement

4.1 General

Following the previous G_E^n measurements [48] we propose to run with 70-80% polarized beam and 4 cm deuteron target. For ^{4}He we plan to adjust the beam current to have the same nucleon luminosity as for the deuteron.

We propose to set the discriminator and HV on the neutron counter of the front and rear detectors to be at 10 MeVee and to trigger the system on a coincidence of the SHMS, front, and rear counters.

For each one of the two Q^2 values we plan two measurements with a deuteron target and two with a ^{4}He target. The two measurements for each target will be with different spin precession (with $\chi = \pm 45°$).

The expected rate and the beam time request are given below.

4.2 Estimation of Signal and Accidental Rates

The constant nucleon luminosity of the experiment (20 μA, 4 cm LD$_2$ target) is:

$$\mathcal{L}_N = 4 \times 10^{37}\,\text{cm}^{-2}\text{sec}^{-1}, \tag{18}$$

which was shown to be viable during experiment E93-038. In deuteron or ^{4}He the (quasi-free) cross section per neutron is:

$$\left.\frac{d\sigma_n}{d\Omega_{e'}}\right|_{QE} = \left.\frac{d\sigma_n}{d\Omega_{e'}}\right|_{E} \cdot A, \tag{19}$$

where $\left.\frac{d\sigma_n}{d\Omega_{e'}}\right|_{E}$ is the elastic electron-neutron cross section, and A is the probability for the neutron to have $|\vec{p}_n| < 100$ MeV/c in the nucleus and be scattered into the neutron polarimeter front detector. A is calculated by a MC which uses the spectral functions for a deuteron and ^{4}He and assumes an isotropic distribution over 4π of the neutron momentum distribution.

The real signal rate is then:

$$R_s = \frac{1}{2}\mathcal{L}_N \left.\frac{d\sigma_n}{d\Omega_{e'}}\right|_{QE} \Omega_{SHMS}\varepsilon^2\eta A_y^2 \tag{20}$$

where $\mathcal{L}_N/2$ is the neutron luminosity, Ω_{SHMS} is the SHMS solid angle (5 msr), ε is the efficiency of the rear and front scintillator array which we assume to be 0.1, A_y is the analyzing power, assumed to be 0.4, η is the attenuation due to the lead shielding ($\eta \sim 0.5$).

The singles electron rate is calculated from scattering off both proton and neutron and is given by:

$$R_e = \mathcal{L}_N \frac{\frac{d\sigma_n}{d\Omega_{e'}}\Big|_E + \frac{d\sigma_n}{d\Omega_{e'}}\Big|_E}{2} \Omega_{SHMS} \tag{21}$$

where $\frac{d\sigma_n}{d\Omega_{e'}}\Big|_E$ is the elastic proton cross section.

The singles neutron rate on the front/rear detectors is estimated based on a calculation done by Pavel Degtiarenko for proposal P05-015 for a 1 μA beam on a 1 cm deuteron target (luminosity of $\sim 6{\cdot}10^{35}$ cm^{-2}sec^{-1}) shown in Fig 9.

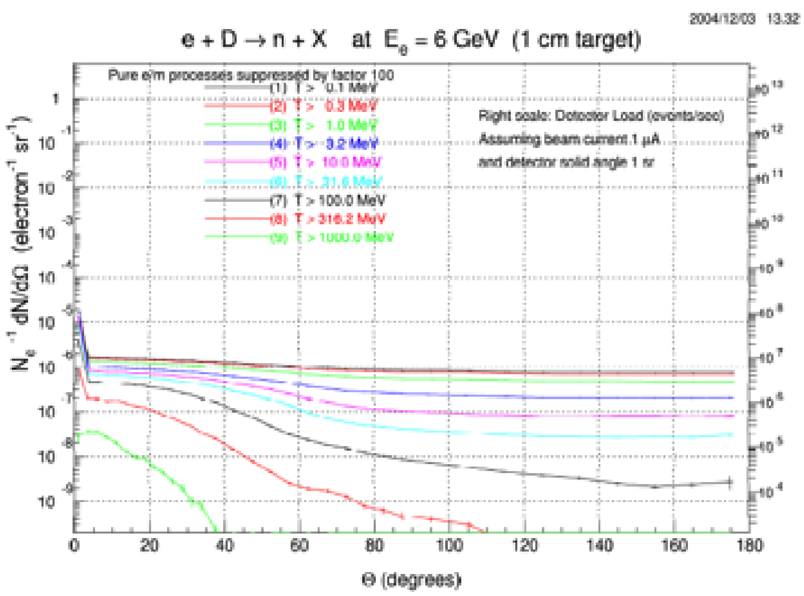

Fig. 9. Calculation of singles neutron rates for a luminosity of $\sim 6{\cdot}10^{35}$ cm^{-2}sec^{-1} and a 1 sr detector.

For a typical angles of 70° and a threshold of 10 MeV the neutrons singles rate is $\sim 2{\cdot}10^6$. For a luminosity of $4{\cdot}10^{37}$ cm^{-2}sec^{-1} and a solid angle of 25 msr, efficiency of 10%, attenuation by the lead wall of 0.5, the expected singles neutron rate on the front detector is:

$$R_f = 2 \cdot 10^6 \cdot \frac{4 \cdot 10^{37}}{6 \cdot 10^{35}} \cdot 25 \cdot 10^{-3} \cdot 0.1 \cdot 0.5 \sim 1.7 \cdot 10^5 \text{Hz} \tag{22}$$

For the rear detector the solid angle is 3 times larger, thus the expected singles rate with similar energy to the signal is $R_r \sim 5.1 \cdot 10^5$ Hz.

4.3 Resolving Time

We assume a time resolution of better than 500 ps for the SHMS and for the front detectors of the polarimeter and a conservative TOF resolution of 2 ns between them. For the TOF the front and rear detectors, we thus assume a conservative resolving time of Δt = 2 ns.

4.4 Random Rates

For signal events the arrival times of the particles to the three detectors (SHSM, front, and rear arrays) are related. Fig 10, taken from ref [48], shows the correlation between the electron-neutron arrival time at the front detector time difference (cTOF), and the front to rear array time difference (rTOF). The signal events are seen at the plot center (cTOF = rTOF = 0 ns). The other event types seen are the different combinations of real and random coincidences between the three detectors.

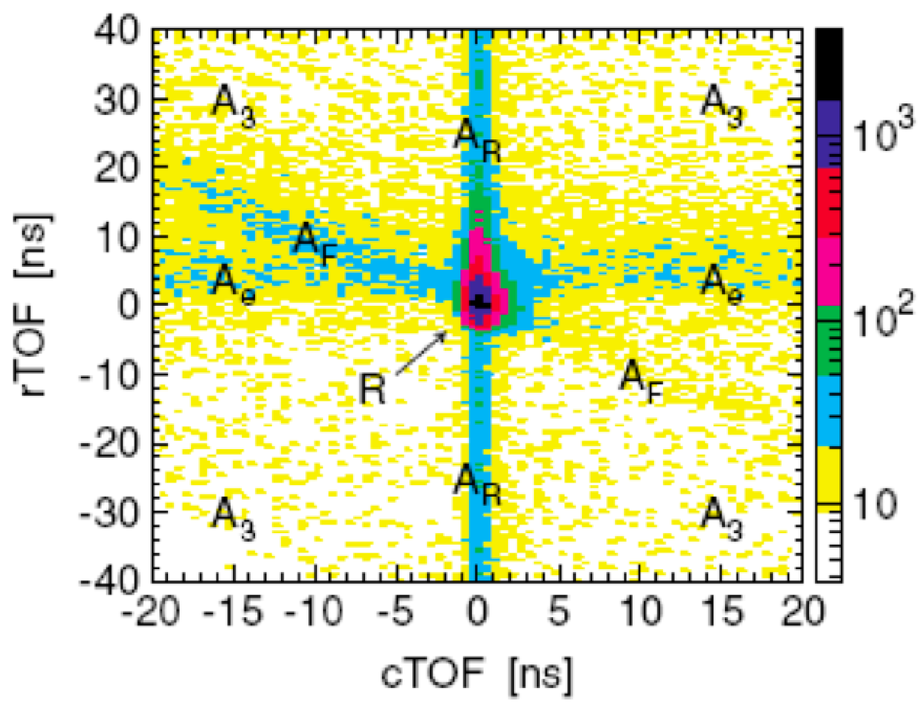

Fig. 10. Correlation between cTOF and rTOF at Q^2 = 1.474 GeV^2. Figure taken from [48].

The equations below estimate the different random coincidence rates within the limits set of the real signal events. These events cannot be separated event-by-event from the signal and need to be subtracted based on an analysis of the background in order to get the signal yield.

Threefold accidental coincidences, denoted A_3, require a random electron in the SHMS, a random neutral particle in the front array, and a random particle in the rear array. They are distributed uniformly over the entire plot. Within the area defined by the real signal events they create a yield of:

$$R_{A_3} = R_e \cdot R_f \cdot R_r \cdot \Delta t^2 \tag{23}$$

Real twofold front-array/rear-array coincidences with an accidental electron are denoted with A_e and are associated with the horizontal band defined by rTOF = 0 ns. Their rate is:

$$R_{A_e} = (R_e \Delta t) \left(R_f^* \cdot \varepsilon A_y^2 \right) \tag{24}$$

where R_f^* is the rate of neutrons with the correct energy for the detected (random) electron. Based on the calculations for the neutron rate we take a conservative estimate of:

$$R_f^*(Q^2 = 0.1\,\mathrm{GeV}^2,\, T_n = 53\,\mathrm{MeV}) = 0.1 \cdot R_f, \text{and} \tag{25}$$
$$R_f^*(Q^2 = 0.4\,\mathrm{GeV}^2,\, T_n = 212\,\mathrm{MeV}) = 0.01 \cdot R_f. \tag{26}$$

Real twofold electron/front-array coincidences with an accidental rear array particle are denoted with A_R and are identified with the vertical band defined by cTOF = 0 ns. The rate for these events is:

$$R_{A_R} = (R_r \cdot \Delta t) \left(\frac{d\sigma_n}{d\Omega_{e'}} \right)_{QE} \cdot \Omega_{SHMS} \cdot \varepsilon\eta \cdot \frac{\mathcal{L}_N}{2} \tag{27}$$

Real twofold electron/rear-array coincidences with an accidental front-array particle are denoted with A_F. These events correspond to events where the hit in the front array need not have been detected but were accompanied by a random hit in the front array in the appropriate time window. The rate for these events may be written as:

$$R_{A_F} = (R_f \cdot \Delta t) \cdot \frac{1}{\varepsilon} R_s \tag{28}$$

Table 2 details the expected rates and the S/B for the two kinematical settings and the two target (deuteron or ^{4}He).

Target	Q^2 (GeV^2)	R_s (sec^{-1})	R_{A_e} (sec^{-1})	R_{A_3} (sec^{-1})	R_{A_R} (sec^{-1})	R_{A_F} (sec^{-1})	$S/(S+B)$
LD_2	0.1	6.96	0.367	0.937	1.78	0.0237	0.69
^{4}He	0.1	0.675	0.367	0.937	1.78	0.0023	0.18
LD_2	0.4	0.798	0.004	0.101	0.204	0.00271	0.72
^{4}He	0.4	0.225	0.004	0.101	0.204	0.0008	0.42

Table 2
Rates and S/B for the two experimental settings.

5 Beam Time Request

The goal of the experiment is to measure a double-ratio with a statistical uncertainty of 1%. Thus, we require a statistical uncertainty of 0.5% for each of the four measurements (2 settings for deuterium and two settings for ^{4}He). The uncertainty on the asymmetry on each measurement is given by:

$$\Delta\mathcal{A} = \sqrt{\frac{2}{N}}, \tag{29}$$

where N is the number of events used for the extraction. For a 0.5% uncertainty we obtain

$$N = 80000. \tag{30}$$

Taking into account the signal-to-background ratio the required number of events is multiplied by $(S+B)/S$. The required number of events may be used to calculated the required beam time. The measurement plan and beam time request are summarized in Table 3.

E_{Beam} (GeV)	Q^2 (GeV^2)	θ_n (deg)	Target	χ (deg)	T (h)
2.2	0.1	76	LD_2	+45	5
2.2	0.1	76	LD_2	-45	5
2.2	0.1	76	^{4}He	+45	185
2.2	0.1	76	^{4}He	-45	185
Enegy + Angle Change					24
6.6	0.4	69	LD_2	+45	39
6.6	0.4	69	LD_2	-45	39
6.6	0.4	69	^{4}He	+45	234
6.6	0.4	69	^{4}He	-45	234

Table 3
Beamtime request for 1% statistical uncertainty of the double-ratio.

The total beam time requested for the physics part of the experiment is 950 hours.

Summary

This letter of intent summarizes our current understanding of the physics interest in the proposed measurement. Also, we explore here the feasibility of performing the measurement at Jefferson Lab. Nevertheless, there is much work to be done before submission to the PAC in proposal form.

A summary of the work to be done follows:

- **Polarimeter design** - as noted (see 3.2) we are exploring two options for the design of the neutron polarimeter. A complete investigation of the advantaged and disadvantages of each of the two proposed designs will be performed. A Monte Carlo analysis of the efficiency and analyzing power of each will be used to select a particular design. Furthermore, we intend to optimize the time resolution of the detectors by using a set of "sandwiched", thin, scintillator bars to replace the thick scintillator bars. This optimization will be investigated for both the front and the rear detector arrays, and a light collection scheme will be developed.
- **Beam Structure** - While currently assuming a CW electron beam, we are also investigating the possibility of using a pulsed, bunched, beam in order to improve timing resolution and backgrounds. Due to the large cross section in the low Q^2 region such a chance will not greatly affect our initial beam time request.
- **Backgrounds** - An investigation of the expected backgrounds will be performed with the dedicated setup proposed in this letter. Methods to reduce the background by optimization of the detector shielding will be explored.
- **Theory Calculations** - Theoretical calculation using the selected kinematics of the experiment will be performed by several theory groups. Using these calculation we will optimize the selected kinematics in order to reduce FSI effects and enhance the expected signal.

Relation to Other Proposals

A similar proposal, using essentially the same technique proposed for this measurement was submitted as proposal PR99-004 to PAC15 and deferred. The PAC report is included in Appendix A.

Clearly the conditions requested by the PAC for resubmission have been fulfilled, viz., experiment E93-049, as well the followup experiment E03-104 have been run [25,29] and have demonstrated significant medium modifications of the proton (Fig. 1).

We note that the PAC recommendation for the case of significant effect is a rapid resubmission of the proposal.This proposal addresses lower Q^2 values than PR99-004, performing this measurement this lower momentum transfer range will allow better theory calculations, higher statistics, and better energy resolution for the recoil neutron.

A PAC15 Report for PR99-004

Proposal: PR-99-004

Scientific Rating: n/a

Title: Medium Modification of Neutron Electromagnetic Form Factors

Spokespersons: J.J. Kelly, R. Madey, P.E. Ulmer

Motivation: The issue of possible changes in the structure of the nucleon in the nuclear medium continues to be of high interest. While arguments based on y-scaling, for example, suggest that these changes cannot be large, high precision measurements of the nucleon form factors in nuclei by entirely different techniques can be important. Measurements and Feasibility: The same apparatus that will be used to measure the ratio of GEn/GMn for the neutron in deuterium in E-93-038 will be used to measure this ratio for a neutron in ^{4}He at a Q^2 of 1 GeV^2. The recoil polarization technique promises small systematic experimental errors. A statistical accuracy of 5% is expected for the polarization ratio P_T/P_L in 14 days. A new ^{4}He target must be designed, constructed, tested, and installed. **Issues:** A comparable experiment to measure the ratio of form factors for the proton in ^{4}He, E93-049, is scheduled for this fall. This experiment is expected to achieve errors of 3 to 5% over the Q^2 range from 1 to 3 GeV^2. The theoretical errors in interpreting the ratio of polarizations in terms of the ratios of form factors are likely to be somewhat smaller for protons than for neutrons. While there are good reasons to carry out measurements for both the neutron and the proton if the medium effects are large, a small effect for the proton is likely to signal a small (and hard to measure) effect for the neutron as well. This experiment should be deferred until initial proton results are available. If the effects seem substantial, rapid resubmission of this proposal is encouraged.

Recommendation: Defer

References

[1] J. J. Aubert *et al.*, Physics Letters B **123**, 275 (1983).

[2] J. Ashman *et al.*, Phys. Lett. **B202**, 603 (1988).

[3] J. Gomez *et al.*, Phys. Rev. D **49**, 4348 (1994).

[4] M. Arneodo *et al.*, Phys. Lett. **B211**, 493 (1988).

[5] M. Arneodo *et al.*, Nucl. Phys. **B333**, 1 (1990).

[6] D. Allasia *et al.*, Phys. Lett. **B249**, 366 (1990).

[7] J. Seely *et al.*, 0904.4448.

[8] D. F. Geesaman, K. Saito and A. W. Thomas, Ann. Rev. Nucl. Part. Sci. **45**, 337 (1995).

[9] P. R. Norton, Reports on Progress in Physics **66**, 1253 (2003).

[10] M. Arneodo, Phys. Rept. **240**, 301 (1994).

[11] G. Piller and W. Weise, Phys. Rept. **330**, 1 (2000), [hep-ph/9908230].

[12] B. Buck and S. M. Perez, Phys. Rev. Lett. **50**, 1975 (1983).

[13] J. Morgenstern and Z. E. Meziani, Phys. Lett. **B515**, 269 (2001), [nucl-ex/0105016].

[14] R. Sawafta *et al.*, Physics Letters B **307**, 293 (1993).

[15] E. Friedman *et al.*, Phys. Rev. C **55**, 1304 (1997).

[16] I. C. Cloët, W. Bentz and A. W. Thomas, Physical Review Letters **102**, 252301 (2009).

[17] N. C. G. P. Zeller, Physical Review Letters **88**, 091802 (2002).

[18] M. Ericson and A. W. Thomas, Phys. Lett. **B128**, 112 (1983).

[19] C. H. Llewellyn Smith, Phys. Lett. **B128**, 107 (1983).

[20] E. L. Berger and F. Coester, Phys. Rev. **D32**, 1071 (1985).

[21] E. E. Sapershtein and M. Z. Shmatikov, JETP Lett. **41**, 53 (1985).

[22] R. L. Jaffe, Comments Nucl. Part. Phys. **13**, 39 (1984).

[23] F. E. Close, R. G. Roberts and G. G. Ross, Phys. Lett. **B129**, 346 (1983).

[24] J. Cleymans and R. L. Thews, Phys. Rev. **D31**, 1014 (1985).

[25] S. Malace, M. Paolone and S. Strauch, AIP Conf. Proc. **1056**, 141 (2008), [0807.2252].

[26] J.-M. Laget, Nucl. Phys. **A579**, 333 (1994).

[27] J. J. Kelly, Phys. Rev. **C59**, 3256 (1999), [nucl-th/9809090].

[28] A. Meucci, C. Giusti and F. D. Pacati, Phys. Rev. **C66**, 034610 (2002), [nucl-th/0205055].

[29] S. Strauch *et al.*, Phys. Rev. Lett. **91**, 052301 (2003).

[30] D.-H. Lu *et al.*, Phys. Lett. **B417**, 217 (1998), [nucl-th/9706043].

[31] D.-H. Lu *et al.*, Phys. Rev. **C60**, 068201 (1999), [nucl-th/9807074].

[32] J. R. Smith and G. A. Miller, Phys. Rev. Lett. **91**, 212301 (2003), [nucl-th/0308048].

[33] J. R. Smith and G. A. Miller, Phys. Rev. **C70**, 065205 (2004), [nucl-th/0407093].

[34] T. Horikawa and W. Bentz, Nucl. Phys. **A762**, 102 (2005), [nucl-th/0506021].

[35] P. Lava, J. Ryckebusch and B. Van Overmeire, Prog. Part. Nucl. Phys. **55**, 437 (2005), [nucl-th/0505005].

[36] I. C. Cloet, W. Bentz and A. W. Thomas, Phys. Lett. **B621**, 246 (2005), [hep-ph/0504229].

[37] R. Schiavilla *et al.*, Phys. Rev. Lett. **94**, 072303 (2005), [nucl-th/0412020].

[38] G. A. Miller, E. Piasetzky and G. Ron, Phys. Rev. Lett. **101**, 082002 (2008), [0711.0972].

[39] I. C. Cloet, G. A. Miller, E. Piasetzky and G. Ron, Phys. Rev. Lett. **103**, 082301 (2009), [0903.1312].

[40] P. L. Chung and F. Coester, Phys. Rev. **D44**, 229 (1991).

[41] A. I. Akhiezer and M. P. Rekalo, Sov. Phys. Dokl. **13**, 572 (1968).

[42] N. Dombey, Rev. Mod. Phys. **41**, 236 (1969).

[43] A. I. Akhiezer and M. P. Rekalo, Sov. J. Part. Nucl. **4**, 277 (1974).

[44] J. J. Kelly, Phys. Rev. **C70**, 068202 (2004).

[45] S. Strauch, Eur. Phys. J. **A19**, 153 (2004), [nucl-ex/0308026].

[46] J. M. Udias *et al.*, Phys. Rev. Lett. **83**, 5451 (1999).

[47] B. D. Anderson *et al.*

[48] B. Plaster *et al.*, Physical Review C (Nuclear Physics) **73**, 025205 (2006).

[49] J. W. Watson *et al.*, Prepared for 11th International Symposium on High-energy Spin Physics and the 8th International Symposium on Polarization Phenomena in Nuclear Physics (SPIN 94), Bloomington, Indiana, 15-22 Sep 1994.

[50] V. D. Efros, W. Leidemann and G. Orlandini, Phys. Lett. **B338**, 130 (1994), [nucl-th/9409004].

[51] V. D. Efros, W. Leidemann, G. Orlandini and N. Barnea, J. Phys. **G34**, R459 (2007), [0708.2803].

[52] N. Barnea, W. Leidemann and G. Orlandini, Nucl. Phys. **A693**, 565 (2001), [nucl-th/0101050].

[53] S. Bacca, N. Barnea, W. Leidemann and G. Orlandini, Phys. Rev. Lett. **102**, 162501 (2009), [0811.4624].